ISSN 2706-655X Vol. 8, Issue 1: 31-37, DOI: 10.25236/IJFET.2026.080105

Position-Sensorless Control of SPMSM Based on Novel Integral SMO

Aoxiang Tian[1,*], Shuaishuai Su[2,3]

[1]*College of Information Science and Engineering, Northeastern University, Shenyang, 110001, China*
[2]*State Key Laboratory of Optical Field Manipulation Science and Technology, Institute of Optics and Electronics, Chinese Academy of Sciences, Chengdu, 610209, China*
[3]*University of Chinese Academy of Sciences, Beijing, 100049, China*
[*]*Corresponding author: 13889182612@163.com*

Abstract: *To address the chattering that often occurs in position-sensorless control systems using sliding-mode observers (SMOs) for surface-mounted permanent-magnet synchronous motors (SPMSMs) at medium and high speeds, this paper proposes an improved integral sliding-mode observer. The traditional discontinuous sign function is replaced by a continuous, smooth saturation function, and the observer is reformulated with a derived algorithm. Using an SPMSM as the test object, both the conventional SMO and the proposed integral SMO are simulated and compared in MATLAB. Results show that the new observer reduces the speed-tracking error to less than 12.5% of that of the conventional SMO, markedly improving accuracy. The proposed method offers stronger speed-tracking capability, enhanced stability, and higher precision, effectively mitigating chattering.*

Keywords: *Novel Integral SMO, SPMSM, Position Sensorless Control, Chattering Suppression*

1. Introduction

Surface-mounted permanent magnet synchronous motors (SPMSMs) are widely applied in industrial automation, transportation, medical equipment, and household appliances because of their high torque density, compact structure, and small size[1,2]. Traditional speed control systems for permanent magnet synchronous motors (PMSMs) rely on mechanical position sensors to obtain real-time rotor position and speed, but these sensors increase manufacturing complexity, size, and cost. To address the expense, structural complexity, and reliability concerns associated with sensors, sensorless control technology has gained growing attention. Instead of using physical sensors, this approach estimates rotor position and speed by analyzing motor currents, voltages, and other operating parameters through advanced control and signal-processing algorithms. By eliminating sensors, sensorless control reduces cost and size while improving the overall reliability and availability of PMSM drive systems[3,4]. Popular sensorless strategies include sliding-mode observers, model reference adaptive schemes, and extended Kalman filters. Among them, sliding-mode variable-structure control is widely used in medium- and high-speed sensorless systems[5]. However, despite its strong theoretical foundation, the sliding-mode observer often suffers from chattering—oscillations of the system state near the sliding surface—when implemented in practice.

At present, methods to eliminate jitter are emerging one after another. authors[6] adopts the continuous saturation switching function sat (x) instead of the traditional discontinuous switching function sign(x), and redefines the sliding mode switching function, which effectively reduces chattering. authors[7] proposed an improved super-helical sliding mode observer, replacing the traditional sgn symbolic function with a continuous tanh(s) function, which enhanced the estimation accuracy of rotational speed and rotor position. authors[8] proposed a PMSM control model based on a novel approach rate sliding mode observer. It introduced a hyperbolic function to replace the traditional switch function and used Kalman filtering to process the low-pass filtered signal, which improved the estimation accuracy of the system. However, further optimization is still needed in complex working conditions. authors [9] proposes a boundary layer design method based on Fuzzy reasoning to construct a Fuzzy Sliding Mode Observer (FSMO). By designing a fuzzy reasoning system, the boundary layer width adaptively changes with the SMO state, improving the observation accuracy. authors [10] In order to alleviate the chattering phenomenon induced by estimated back-EMF as well as phase delay caused by a low-pass filter that are inherent in conventional SMOs, a super-twisting algorithm based SMO (STA-

ISSN 2706-655X Vol. 8, Issue 1: 31-37, DOI: 10.25236/IJFET.2026.080105

SMO) with a modified phase-locked loop (PLL) is adopted to precisely estimate the angular position and angular speed of a SPMSM. Simulation results verify the effectiveness of the proposed rotor position estimation method.

This paper proposes a novel integral sliding mode observer, which replaces the traditional signed function with a continuous saturation function to weaken chatters and improve accuracy. Finally, the accuracy of the proposed method was verified through simulation experiments.

2. SPMSM Mathematical Model and Conventional Sliding Mode Observer

2.1 SPMSM Mathematical Model

At present, according to the different positions on the permanent magnet rotor, the rotor structure of three-phase PMSM can be divided into two types of structures: surface-mounted and built-in, as shown in Fig. 1.

Fig. 1 Rotor structure of a three-phase PMSM

The surface-mounted rotor structure has the advantages of simple structure, low manufacturing cost and small rotational inertia, so the surface-mounted permanent magnet synchronous motor is chosen as the study in this paper. The rotor of SPMSM adopts the hidden-pole structure, and its intersection and straight-axis inductances are approximately equal (Ld≈Lq), which leads to the multivariate, strong coupling and nonlinear problems of the mathematical model in the traditional three-phase static coordinate system (abc), so it is necessary to carry out the Clark transformation to transform the SPMSM mathematical model under the ABC coordinate system to the α-β coordinate system, so as to realize the decoupling of the motor mathematical model[11].

The stator equation under the α-β coordinate system can be expressed as follows[12]:

$$\begin{bmatrix} u_\alpha \\ u_\beta \end{bmatrix} = R_s \begin{bmatrix} i_\alpha \\ i_\beta \end{bmatrix} + L_s \frac{d}{dt} \begin{bmatrix} i_\alpha \\ i_\beta \end{bmatrix} + \begin{bmatrix} e_\alpha \\ e_\beta \end{bmatrix} \tag{1}$$

of which:

$$\begin{bmatrix} e_\alpha \\ e_\beta \end{bmatrix} = \omega_e \psi_f \begin{bmatrix} -\sin\theta_e \\ \cos\theta_e \end{bmatrix} \tag{2}$$

$$\frac{d}{dt}\begin{bmatrix} i_\alpha \\ i_\beta \end{bmatrix} = \frac{1}{L_d}\begin{bmatrix} -R_s & 0 \\ 0 & -R_s \end{bmatrix}\begin{bmatrix} i_\alpha \\ i_\beta \end{bmatrix} + \frac{1}{L_d}\begin{bmatrix} u_\alpha \\ u_\beta \end{bmatrix} - \frac{1}{L_d}\begin{bmatrix} e_\alpha \\ e_\beta \end{bmatrix} \tag{3}$$

of which: $[u_\alpha \quad u_\beta]^T$, $[i_\alpha \quad i_\beta]^T$ Respectively, the stator voltage and stator current in the stationary coordinate system - Lu Xia, R is the stator resistance, ω_e is the angular velocity, ψ_f represents the magnetic flux of the permanent magnet.

2.2 Traditional integral sliding mode observer design

In a three-phase surface-mounted PMSM control system, the back EMF of the permanent magnet synchronous motor determines the speed and rotor position angle. By rewriting the voltage equation in equation (1) into a current equation form, the current state equation in the α-β coordinate system is

ISSN 2706-655X Vol. 8, Issue 1: 31-37, DOI: 10.25236/IJFET.2026.080105

obtained as:

$$\begin{cases} \dfrac{di_\alpha}{dt} = -\dfrac{R}{L}i_\alpha - \dfrac{1}{L}e_\alpha + \dfrac{1}{L}u_\alpha \\ \dfrac{di_\beta}{dt} = -\dfrac{R}{L}i_\beta - \dfrac{1}{L}e_\beta + \dfrac{1}{L}u_\beta \end{cases} \tag{4}$$

Traditional SMO are typically designed as follows:

$$\begin{cases} \dfrac{d\hat{i}_\alpha}{dt} = -\dfrac{R}{L}\hat{i}_\alpha - \dfrac{1}{L}\tau_\alpha + \dfrac{1}{L}u_\alpha \\ \dfrac{d\hat{i}_\beta}{dt} = -\dfrac{R}{L}\hat{i}_\beta - \dfrac{1}{L}\tau_\beta + \dfrac{1}{L}u_\beta \end{cases} \tag{5}$$

$\hat{i}_\alpha, \hat{i}_\beta$ represent the estimated values of the stator current, respectively, τ_α, τ_β a disturbance estimation term introduced into the sliding mode observer to replace the back EMF that cannot be measured directly.

Subtracting equation (8) from equation (7) yields the following error equation for the stator current:

$$\begin{cases} \dfrac{d\tilde{i}_\alpha}{dt} = -\dfrac{R}{L}\tilde{i}_\alpha - \dfrac{1}{L}\tau_\alpha + \dfrac{1}{L}e_\alpha \\ \dfrac{d\tilde{i}_\beta}{dt} = -\dfrac{R}{L}\tilde{i}_\beta - \dfrac{1}{L}\tau_\beta + \dfrac{1}{L}e_\beta \end{cases} \tag{6}$$

of which: $\tilde{i}_\alpha = \hat{i}_\alpha - i_\alpha, \tilde{i}_\beta = \hat{i}_\beta - i_\beta$ representing the current estimation error in the α-axis and β-axis directions, respectively.

In this study, an integral sliding surface structure is used, which has good results in handling steady-state errors and suppressing high-frequency oscillations. Its mathematical expression is as follows:

$$s = \begin{bmatrix} s_\alpha \\ s_\beta \end{bmatrix} = \begin{bmatrix} \tilde{i}_\alpha + C\int \tilde{i}_\alpha dt \\ \tilde{i}_\beta + C\int \tilde{i}_\beta dt \end{bmatrix} \tag{7}$$

of which, C is the positive sliding mode gain coefficient.

The designed sliding mode control ratio is as follows:

$$\begin{bmatrix} \tau_\alpha \\ \tau_\beta \end{bmatrix} = \begin{bmatrix} \varepsilon \mathrm{sgn}(s_\alpha) \\ \varepsilon \mathrm{sgn}(s_\beta) \end{bmatrix} \tag{8}$$

of which, ε is the switching gain, and $sgn(\cdot)$ denotes the sign function.

In a sliding mode observer, when the system state variables reach and remain near the sliding surface, the observation error tends to be minimal, and the system dynamics tend to the ideal trajectory. The control quantity at this point can be regarded as an equivalent control quantity, thereby establishing the following electromotive force estimation model:

$$\begin{bmatrix} e_\alpha \\ e_\beta \end{bmatrix} = \begin{bmatrix} \tau_\alpha \\ \tau_\beta \end{bmatrix} = \begin{bmatrix} \varepsilon\, \mathrm{sgn}(s_\alpha) \\ \varepsilon\, \mathrm{sgn}(s_\beta) \end{bmatrix} \tag{9}$$

ISSN 2706-655X Vol. 8, Issue 1: 31-37, DOI: 10.25236/IJFET.2026.080105

3. New Type of Integral Sliding Mode Observer

3.1 Design of a New Type of Integral Sliding Mode Observer

The traditional sliding mode control method usually adopts symbolic functions as the control law. However, the discontinuity of signed functions often leads to sliding mode chattering in practical applications. To solve this problem, one effective strategy is to adopt a smooth activation function instead of the traditional symbolic function.

This paper proposes a smooth saturation function that can provide smooth transition characteristics and help suppress the chattering phenomenon caused by the switching of symbolic functions. Its mathematical expression is:

$$T\left(x\right)=1-\frac{2}{e^{ax}+1} \tag{10}$$

As the parameter a increases, the saturation function gradually approaches the sign function, making the system more susceptible to high-frequency sliding-mode chatter. Conversely, when a is too small, the boundary layer becomes excessively wide, which suppresses chattering but markedly lowers the control gain. This reduction weakens the system's resistance to external disturbances and parameter uncertainties, and may even compromise the attractiveness of the sliding surface, leading to steady-state errors or dynamic instability, as illustrated in Fig. 2.

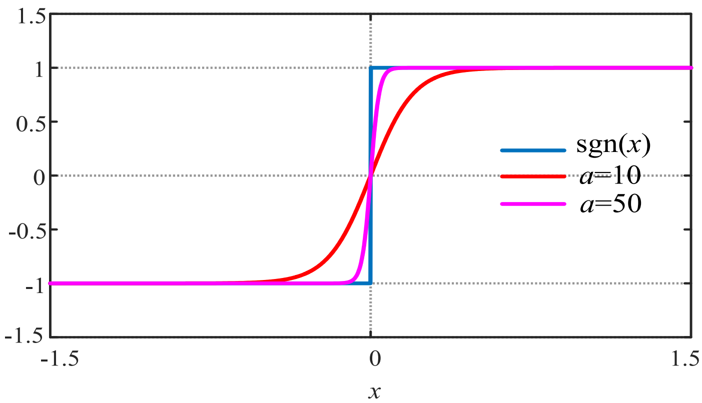

Fig. 2 Saturation function graph

This paper still selects equation (10) as the sliding mode switching surface, and the improved sliding mode convergence rate is as follows:

$$\begin{bmatrix}\tau_\alpha \\ \tau_\beta\end{bmatrix}=\begin{bmatrix}\varepsilon T(s_\alpha) \\ \varepsilon T(s_\beta)\end{bmatrix} \tag{11}$$

Combining Equations (8), (10), and (14) yields the improved sliding mode observer algorithm:

$$\begin{cases}\dfrac{d\hat{i}_\alpha}{dt}=-\dfrac{R}{L}\hat{i}_\alpha-\dfrac{1}{L}\varepsilon T\left(s_\alpha\right)+\dfrac{1}{L}u_\alpha \\ \dfrac{d\hat{i}_\beta}{dt}=-\dfrac{R}{L}\hat{i}_\beta-\dfrac{1}{L}\varepsilon T\left(s_\beta\right)+\dfrac{1}{L}u_\beta\end{cases} \tag{12}$$

Subtracting equation (15) from equation (7) yields the improved stator current estimation equation for the motor:

$$\begin{cases}\dfrac{d\tilde{i}_\alpha}{dt}=-\dfrac{R}{L}\tilde{i}_\alpha-\dfrac{\varepsilon}{L}T(s_\alpha)+\dfrac{1}{L}e_\alpha \\ \dfrac{d\tilde{i}_\beta}{dt}=-\dfrac{R}{L}\tilde{i}_\beta-\dfrac{\varepsilon}{L}T(s_\beta)+\dfrac{1}{L}e_\beta\end{cases} \tag{13}$$

ISSN 2706-655X Vol. 8, Issue 1: 31-37, DOI: 10.25236/IJFET.2026.080105

Similarly, we obtain the equivalent control expression for the counter-electromotive force:

$$\begin{bmatrix} e_\alpha \\ e_\beta \end{bmatrix} = \begin{bmatrix} \varepsilon T(s_\alpha) \\ \varepsilon T(s_\beta) \end{bmatrix} \tag{14}$$

Substitute the estimated back EMF into the specific position and rotational speed equations to obtain specific parameters. The specific expressions for the angle and angular velocity are as follows:

$$\hat{\theta}_{eq} = -\arctan\left(\frac{\varepsilon T(s_\alpha)}{\varepsilon T(s_\beta)}\right) \tag{15}$$

$$\omega_e = \frac{\sqrt{\left(\varepsilon T(s_\alpha)\right)^2 + \left(\varepsilon T(s_\beta)\right)^2}}{\varphi_l} \tag{16}$$

4. Simulation Comparison of Two Observer

To evaluate the performance of the proposed integral SMO, a sensorless control model for a permanent magnet synchronous motor was developed in Simulink. In the simulation, the parameter a in the saturation function T(*x*) was set to 40. The PMSM specifications are listed in Table 1. A variable-step solver ode45 was used, with the reference speed initialized at 600 r/min and increased to 1000 r/min at 0.05 s. The motor operated under no-load conditions.

Table 1 Parameters of permanent magnet synchronous motor

Motor parameters	Numerical value
pn	4
RS/Ω	2.875
Ls/h	0.0085
Ψf/wb	0.175
J/(kg.m2)	0.001
B	0

The back EMF carries essential information about rotor position and speed. The more accurately it is estimated, the better the sliding-mode observer performs. Fig. 3 and 4 show the α- and β-axis back EMFs after low-pass filtering for the conventional sliding-mode observer, alongside those obtained using the improved observer.

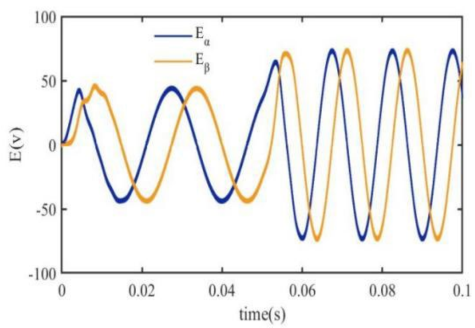

Fig. 3 Conventional SMO back EMF

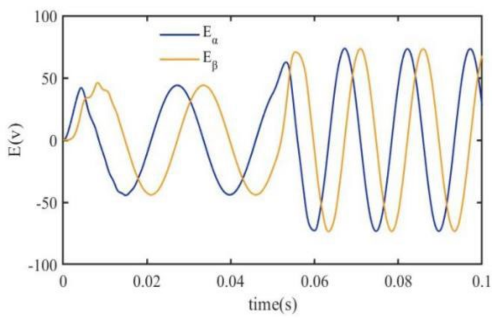

Fig. 4 New integrated SMO back EMF

The speed tracking simulation diagrams of the traditional SMO and novel integral SMO for the first 0.1 seconds were respectively captured. The simulation experiment results are shown in Figures 4 and 5.

ISSN 2706-655X Vol. 8, Issue 1: 31-37, DOI: 10.25236/IJFET.2026.080105

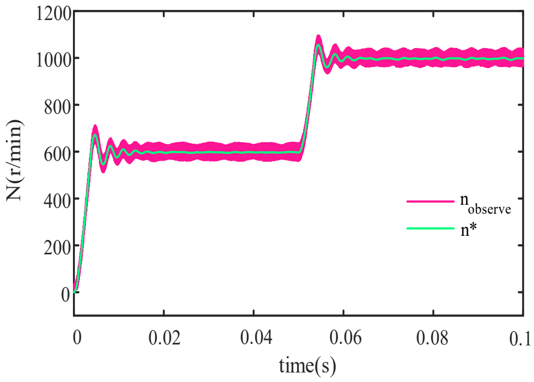

Fig. 5 Conventional SMO speed tracking

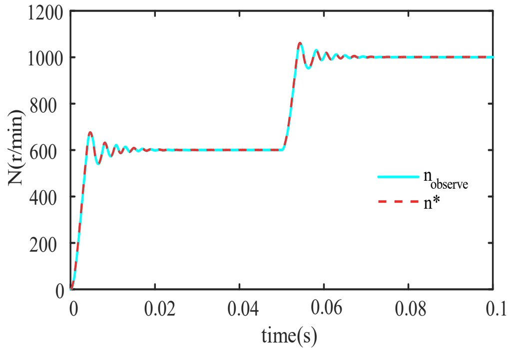

Fig. 6 Novel integral SMO speed tracking

As can be seen from Fig. 5, n* and $n_{observer}$ are the actual and observed rotational speeds respectively under the traditional sliding mode observer. During the start-up stage, that is, the first 0.02 seconds, the actual rotational speed responds faster, while $n_{observer}$ has a significant lag compared to n*. When the rotational speed stabilizes at 600r/min and 1000r/min, n* fluctuates slightly at the steady-state value, while $n_{observer}$ fluctuates significantly at the steady-state value.

As can be seen from Fig. 6, when the rotational speed stabilizes at 600r/min and 1000r/min, the $n_{observer}$ obtained by novel integral SMO can significantly track n*, and its fluctuation amplitude is smaller, approaching the actual value.

Fig. 7 compares the rotational speed error of the traditional sliding mode observer with that of novel integral SMO.

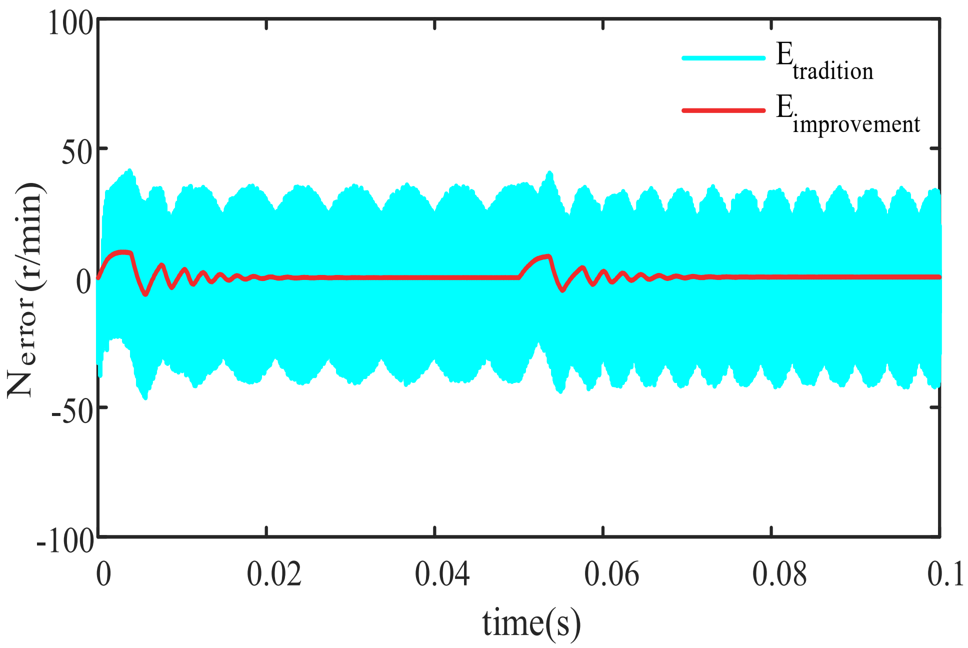

Fig. 7 shows the rotational speed error before and after improvement

As shown in Fig. 7, $E_{traditional}$ denotes the speed error of the traditional sliding-mode observer, while $E_{improvement}$ represents that of the proposed integral SMO. For $E_{tradition}$, the maximum error is 40.8 and the minimum is 18, indicating a wide fluctuation range. For $E_{improvement,}$ the maximum error is 5.15 and the minimum is 1.4; larger oscillations appear before 0.02 s, but once steady state is reached, the error approaches zero with only minor variations. Compared with the conventional observer, the proposed method reduces the speed-tracking error to less than one-eighth of the original value, markedly enhancing the dynamic performance and reliability of sensorless control. These results confirm that the improved sliding-mode observer achieves excellent speed-control accuracy in closed-loop applications.

ISSN 2706-655X Vol. 8, Issue 1: 31-37, DOI: 10.25236/IJFET.2026.080105

5. Conclusion

This study investigates a surface-mounted permanent magnet synchronous motor and addresses the pronounced chattering and large speed-estimation error of conventional sliding-mode observers. A novel integral sliding-mode observer is proposed, replacing the discontinuous sign function sgn(x) with a continuous saturation function $T(x)$. Sensorless control systems based on both the conventional and improved observers were modeled and simulated for comparison. Results demonstrate that the proposed observer, operating with a continuous saturation function, effectively suppresses chattering and tracks the rotor speed with much higher precision. Compared with the traditional approach, the integral SMO achieves substantially lower speed-estimation error, enhancing both accuracy and stability. Simulation results confirm the feasibility of the method, offering improved performance for sensorless PMSM control. This design also has some limitations, the effectiveness of the new integral sliding mode observer is only verified by simulation, and the physical verification is not carried out.

References

[1] Chai Chenglong, Li Juan, Li Shengquan, et al. All-digital fuzzy control without speed sensor based on the sliding mode observer design [J]. Journal of nanjing information engineering university, 2024 (5) : 710-716.

[2] Gan Chun, Qu Ronghai, Shi Haochen, et al. A Review of All-Domain High-Efficiency Operation Control Strategies for Wide Speed Regulation Permanent Magnet Synchronous Motors [J]. China Motor Journal of Engineering,2023,43(7):2496-2512.

[3] GE Y, SONG W, YANG Y, et al. A polar-coordinate-multi-signal flux-observer based PMSM non-pll sensorless control[J].IEEE Transactions on Power Electronics, 2023, 38(9) : 10579-10583.

[4] Gong C, Hu Y H, Gao J Q, et al. An improved delay-suppressed sliding-mode observer for sensorless vector controlled PMSM[J]. IEEE Transactions on Industrial Electronics, 2020, 67(7): 5913-5923

[5] Lu Fei, Zhang Keke, Gong Miao, et al. Based on second order approximation of EKF sensorless control strategy of permanent magnet synchronous motor [J]. Micro &special motor, 2024,52 (5) : 65-69. The DOI: 10.20026 / j.carol carroll nki ssemj. 2024.0064.

[6] Gao Ziyuan. Research on PMSM Control System Based on Sliding Mode Observer [D]. Huainan: Anhui University of Science and Technology, 2019.

[7] Xing Xiaoke, Chi Yaodan, Lin Guangbin, et al. Control of Permanent Magnet Synchronous Motor based on Improved sliding Mode Observer [J]. Electrical Industry,2025,(05):12-16+23.

[8] Sun Huifang, Liu Xiaochun. Based on new near rate sliding mode observer of permanent magnet synchronous motor control research [J]. Automation and instrumentation, 2025, (03) : 81-84. The DOI: 10.14016 / j.carolcarrollnki.1001-9227.2025.03.081.

[9] Ju Jintao, Zhao Shiwei, Yang Xiangyu. Position sensorless control of PMSM Based on Fuzzy Sliding Mode Observer [J/OL]. Micro Motors,1-7[2025-07-18].https://doi.org/10.15934/j.cnki.micromotors. 20250711.001.

[10] J. -P. Chang and M. -Y. Cheng, "Rotor Position Estimation for a Position-Sensorless FOC PMSM Drive—A Super-Twisting-Based Sliding Mode Observer Approach," in IEEE Access, vol. 13, pp. 164540-164551, 2025.

[11] Yuan Lei, Hu Bingxin, Wei Keyin, et al. Control Principle and MATLAB Simulation of Modern Permanent Magnet Synchronous Motor [M]. Beijing Aerospace Press: Haidian District, Beijing,2015:1-279.

[12] B. Wang, Y. Shao, Y. Yu, Q. Dong, Z. Yun and D. Xu, "High-Order Terminal Sliding-Mode Observer for Chattering Suppression and Finite-Time Convergence in Sensorless SPMSM Drives," in IEEE Transactions on Power Electronics, vol. 36, no. 10, pp. 11910-11920, Oct. 2021.